Microsc. Microanal. Microstruct. **6** (1995) 141–147 FEBRUARY **1995**, PAGE 141

Classification
Physics Abstracts
61.70T — 61.80J — 61.16D

In Situ EELS and TEM Observation of Al Implanted with Nitrogen Ions

Kiichi Hojou([1]), Shigemi Furuno([1]), Tesuo Tsukamoto([2]), Kouhei N. Kushita([1]), Hitoshi Otsu([1]) and Kazuhiko Izui([3])

([1]) Japan Atomic Energy Research Institute, Tokai-mura, Ibarabi-ken, 319-11, Japan
([2]) Origin Electric Co. Ltd., 1-18-1, Takada, Toshima-ku, Tokyo 171, Japan
([3]) Nagasaki Univ., Bunkyo-machi, Nagasaki-si, Nagasaki, 852, Japan

(Received July 27, 1994; accepted January 3, 1995)

Abstract. — Formation processes of Aluminum nitride (AlN) in Aluminum (Al) implanted with nitrogen were examined by *in situ* EELS and TEM observations during nitrogen ion implantation in an electron microscope at room temperature and 400 °C. AlN phase was identified both by EDP and EELS after nitrogen ion implantation to 6×10^{20} $(N^+)/m^2$. The observed peak (20.8 eV) in EELS spectra was identified as the plasmon loss peak of AlN formed in Al. The binding energy of N_{1s} in Al was found to shift by about 4 eV to the lower side with increasing nitrogen-ion fluence. Unreacted Al was also found to remain in the AlN films after high fluence implantation both at room temperature and 400 °C.

1. Introduction

Aluminum nitride (AlN) is of particular interest because of its extreme hardness, high melting point, good thermal conductivity and stability up to very high temperature. Furthermore, AlN has a large energy gap, good dielectric properties for active and passive components in semiconductor device and chemical inertness. AlN films can be formed by chemical vapor deposition [1], reactive sputter deposition [2] and ion implantation [3]. In particular, ion implantation may be used as a low temperature and well-controlled technique for changing the surface properties of materials as well as for forming metastable alloys and chemical compounds [4].

The synthesis of AlN performed by nitrogen implantation at room temperature or above has been reported by Pavlov *et al.* [3] and other various researchers [5, 6]. In contrast, Bykov *et al.* [7] were unable to detect AlN after nitrogen implantation at both low (−100 °C) and high (100 and 200 °C) temperatures. Furuno *et al.* [8] showed that no AlN crystallite was formed by 20 keV nitrogen implantation below 150 °C. There are some differences among the results in the literatures about the formation of AlN after ion implantation.

The present paper reports the results of *in-situ* observation and analysis by parallel-electron energy loss spectrometer (P-EELS) about the formation of AlN during nitrogen molecule ion implantation into aluminum.

2. Experimental

Polycrystalline aluminum films with a thickness of about 100 nm were made in the following way: aluminum was deposited onto cleaved NaCl surface heated at 300 °C under the vacuum of 1×10^{-6} Torr. They were then floated off on water and picked up on Ti grids. *In-situ* EELS analysis and transmission electron microscopic (TEM) observation during ion implantations were performed with a system consisting of a 400 kV TEM (JEM-4000FX; JEOL Ltd.) connected with two ion accelerators (TIB-40; Origin Electric Ltd.) and P-EELS (Model-666; Gatan Inc.) [9]. In the present experiments, ion implantations were performed with 30 keV N_2^+ ions at a flux of 2×10^{18} $(N^+)/m^2s$ at room temperature and 400 °C. The vacuum level during ion implantations was less than 1×10^{-7} Torr. The TEM and EELS analysis were operated at 150 kV to avoid the damage in the specimens by electrons.

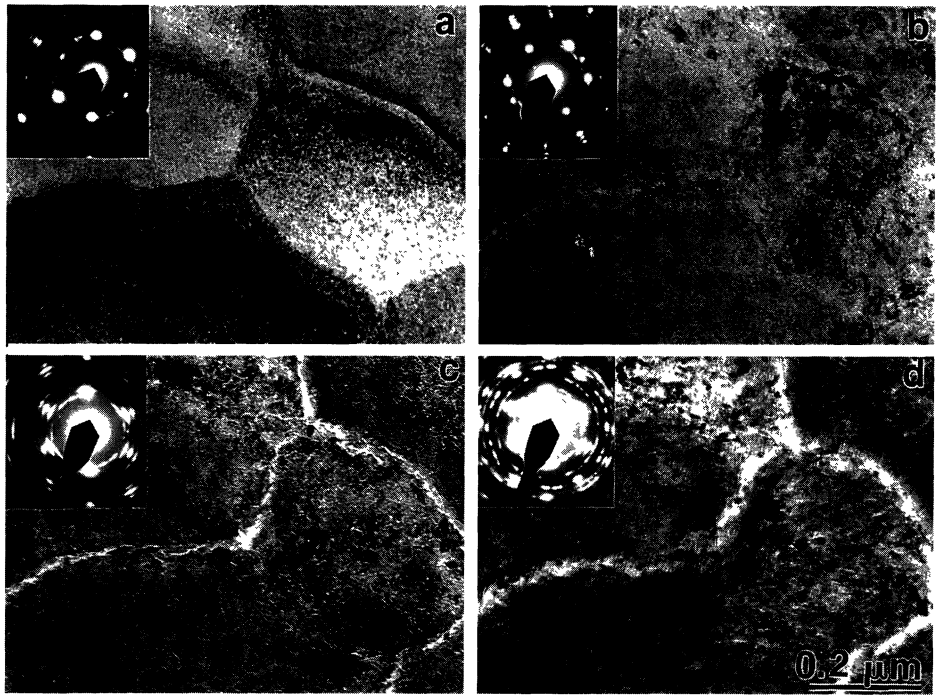

Fig. 1. — Structural changes in polycrystalline Al during 30 kV N_2^+ ion implantation with a flux of 2×10^{18} $(N^+)/m^2s$ at RT. Fluence: a) 6×10^{20}, b) 1.2×10^{21}, c) 1.8×10^{21}, d) 2.4×10^{21} $(N^+)/m^2$.

3. Results and Discussion

3.1 IMPLANTATION AT ROOM TEMPERATURE. — Figures 1a to d show the results of both *in-situ* TEM observations and the electron diffraction patterns (EDP) in the process of formation of AlN in aluminum. These figures show that at the implantation fluence of about 1×10^{19} $(N^+)/m^2$, black spots appeared and then increased in number with the increasing fluence. Depth distribution of

ions and damage density due to nitrogen-ion implantations into aluminum were calculated by the TRIM computer code. The penetration depth of the implanted 30 keV N_2^+ ions in aluminum was estimated to be about 90 nm, and the depth of damage was calculated to be about 70 nm. The black spots occurred within the range of implanted ions. In this experiments, as the specimens used here were Al films with a thickness of about 100 nm, the ion implantation affected thorough the entire samples.

Table I. — *Summary of the experimental interplanar spacing ($d_{exp.}$-value) obtained into aluminum during nitrogen ion implantation with a flux of* 2×10^{18} *$(N^+)/m^2s$ at RT. (hkl, Miller indices of lattice planes; hkil, Miller-Bravais indices of lattice planes; d_{th}, theoretical interplanar spacing; $d_{exp.}$, experimental interplanar spacing).*

hkl	hkil	d_{th}(nm)	Phase	d_{exp}(nm)			N/m^2
				6×10^{20}	1.2×10^{21}	1.8×10^{21}	2.4×10^{21}
001		0.3922	Al_2O_3				
	$01\bar{1}0$	0.2702	AlN	0.287			0.268
	0002	0.2495	AlN	0.254	0.258	0.258	0.248
	$01\bar{1}1$	0.2376	AlN		0.239	0.239	
111		0.2333	Al	0.225			0.234
(222)		0.2287	AlN_c		0.227		
012		0.2082	Al_2O_3			0.206	0.206
200		0.2021	Al				0.202
002		0.1961	Al_2O_3			0.196	
	$01\bar{1}2$	0.1833	AlN				0.181
022		0.1737	Al_2O_3	0.175	0.175	0.175	
	$11\bar{2}0$	0.1560	AlN				0.154
233		0.1508	Al_2O_3		0.148		
220		0.1429	Al	0.147			
	$01\bar{1}3$	0.1417	AlN		0.141		
013		0.1402	Al_2O_3		0.138		0.139
	$02\bar{2}0$	0.1351	AlN	0.137		0.136	
023		0.1334	Al_2O_3				0.133
	$02\bar{2}1$	0.1304	AlN		0.129	0.130	0.131
224		0.1273	Al_2O_3	0.127			
	0004	0.1247	AlN		0.126		0.126
311		0.1219	Al				
	$02\bar{2}2$	0.1188	AlN		0.118	0.118	0.118
222		0.1167	Al				

It was found in EDP that additional spots and rings appeared newly during ion implantations at room temperature. The $d_{exp.}$-values (experimental interplanar spacing) obtained from these spots and rings are listed in Table I, where $d_{th.}$-values (theoretical interplanar spacing) are quoted from Rauchenbach *et al.* [6]. The values agreed with those obtained in the present experiment. From these results, the film formed newly on the specimen can be identified to be AlN of hcp type, and the lattice parameters of this unit cell were determined as: $a = 0.314$ nm and $c = 0.506$ nm.

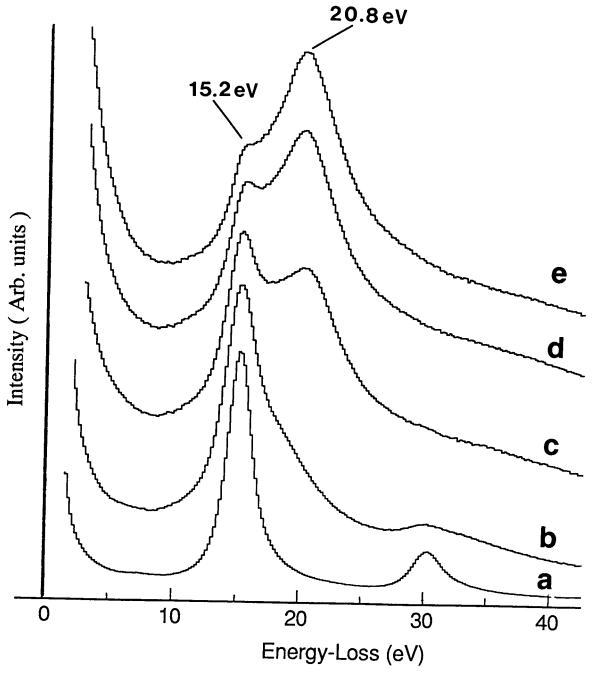

Fig. 2. — Change of plasmon loss spectra from Al during 30 kV N_2^+ ion implantation with a flux of 2×10^{18} $(N^+)/m^2s$ at RT. Fluence: a) unimplanted, b) 6×10^{20}, c) 1.2×10^{21}, d) 1.8×10^{21}, e) 2.4×10^{21} $(N^+)/m^2$.

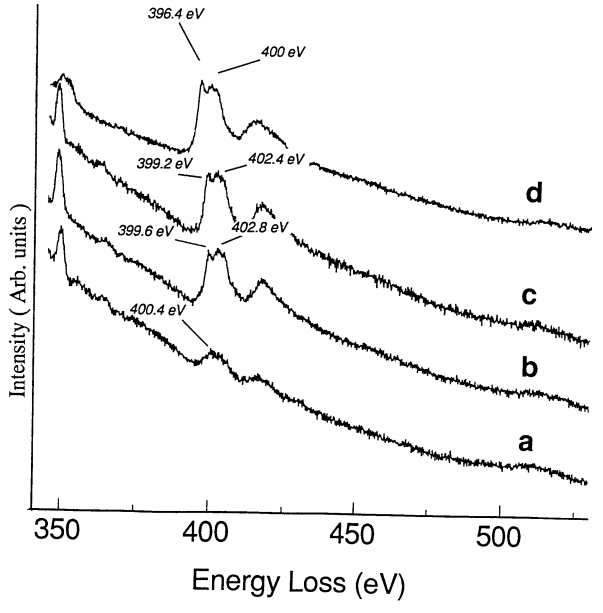

Fig. 3. — Change of N_{1s} edges from Al during 30 kV N_2^+ ion implantation with a flux of 2×10^{18} $(N^+)/m^2s$ at RT. Fluence: a) 6×10^{20}, b) 1.2×10^{21}, c) 1.8×10^{21}, d) 2.4×10^{21} $(N^+)/m^2$.

Table I also indicate that Al_2O_3 phase appeared in addition to AlN by nitrogen implantation at room temperature. Al_2O_3 is considered to be formed by irradiation-induced chemical reaction of Al with oxygen absorbed in Al prior to the implantation. Figures 2a to e show the changes of plasmon loss spectra of aluminum film with increasing nitrogen-ion fluences. Figure 2a shows the P-EELS spectrum obtained from unimplanted aluminum film. The two peaks at 15 eV and 30 eV are the first and second plasmon loss peaks of aluminum. Figures 2b to e show P-EELS spectra obtained after ion implantations to the fluence of 6×10^{20} to 2.4×10^{21} $(N^+)/m^2$. The observed peak (20.8 eV) in these spectra are clearly recognized as the plasmon loss peaks of AlN formed in aluminum by comparing then with that of a standard AlN sample. In this experiment, the matrix and grain boundary were found to be thinned by physical sputtering. Figure 3a to d show the spectra of N_{1s} measured by P-EELS as a function of the fluence of implanted nitrogen ions. These spectra were found to shift to the lower energy side with the increasing nitrogen-ion fluence. The observed N_{1s} (396.4 eV) spectrum agreed with the binding energy of AlN [10, 11], indicating that nitrogen was bound to aluminum in the form of AlN. The energy value of about 400 eV in the N_{1s} spectra for the low fluence case, shown in Figure 3a, was recognized to correspond to the adsorbed nitrogen in aluminum, as proposed by Raole *et al.* [11]. However, the plasmon loss peak of Al_2O_3 (about 23 eV) and O_{1s} spectra were not found in the spectra, as shown in Figures 2 and 3.

3.2 IMPLANTATION AT 400 °C. — Figures 4a to d show the results of both TEM observation and EDP in the process of formation of AlN in aluminum at 400 °C. The diameter of the AlN precipitates grew with an increasing nitrogen fluence. Furthermore, the EDP clearly shows that AlN and Al_2O_3 are present in Al. The EDP shows that additional spots and rings appear newly during ion implantation at 400 °C. The $d_{exp.}$-values obtained from these spots and rings are listed in Table II, where $d_{th.}$-values are quoted from Rauchenbach *et al.* [6] and in agreement with those obtained in the present experiment. From these results, the film newly formed on the specimen at 400 °C can be identified to be AlN of hcp type, and the lattice parameters of this unit cell were determined to be that: $a = 0.310$ nm and $c = 0.506$ nm. In Figure 4c, the strong diffraction rings appeared at a fluence of about 1.8×10^{21} $(N^+)/m^2$ at 400 °C. The intensity of these rings increased with an increasing ion fluence, and these rings were identified to be of Al_2O_3 by diffraction analysis. The Al_2O_3 are considered to be formed from the stronger effects of both high temperature (400 °C) and irradiation induced chemical reaction of Al than these in the room-temperature implantation experiments. Figures 5a to e show the changes of the plasmon loss spectrum of aluminum film with the nitrogen ion fluences. The big peaks (21 eV) shown in Figures 5d and e are clearly recognized as the plasmon loss peaks of AlN, which are identical peaks with the peak shown in Figure 2e.

Although Al_2O_3 was detected by EDP during high temperature implantation, it could not be detected by the plasmon loss spectra in EELS. The reason for this difference can be ascribed to the experimental condition that the peaks of AlN (at 21 eV) and Al_2O_3 (at 23 eV) could not be discriminated by our EELS. Unreacted Al was also found to remain in the AlN films at high temperature.

4. Conclusions

Aluminum samples were observed by *in situ* EELS and TEM during N_2^+ ion implantations.

EDP profile indicated the formation of AlN in aluminum samples both at room temperature and 400 °C. The formation of AlN was also identified by the plasmon-loss as well as core-loss profiles of EELS spectra after nitrogen ion implantation to 6×10^{20} $(N^+)/m^2$.

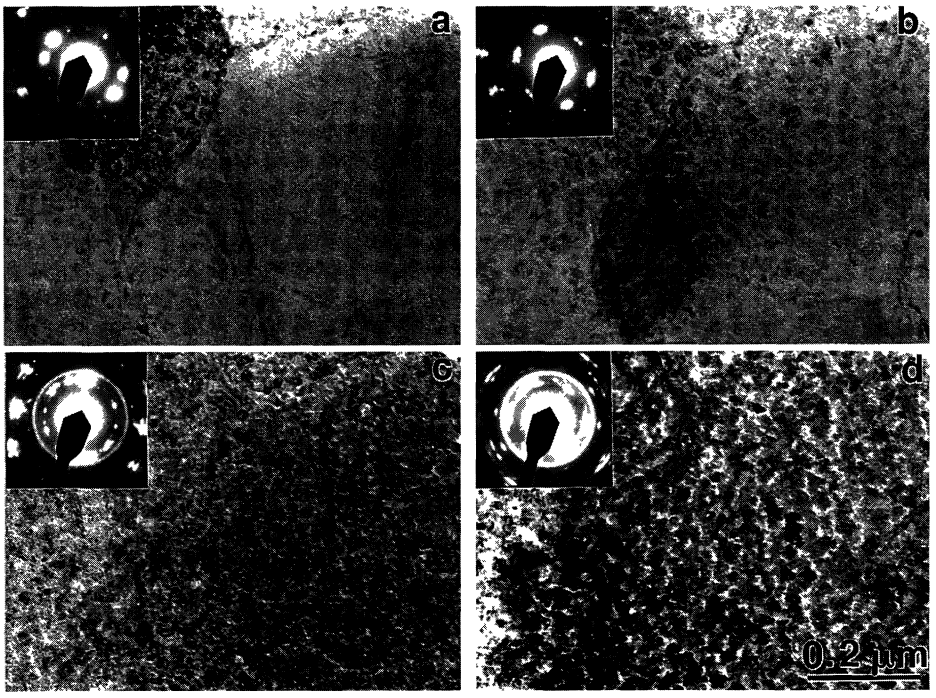

Fig. 4. — Structural changes in Al during 30 kV N_2^+ ion implantation with a flux of 2×10^{18} $(N^+)/m^2s$ at 400 °C. Fluence: a) 6×10^{20}, b) 1.2×10^{21}, c) 1.8×10^{21}, d) 2.4×10^{21} $(N^+)/m^2$.

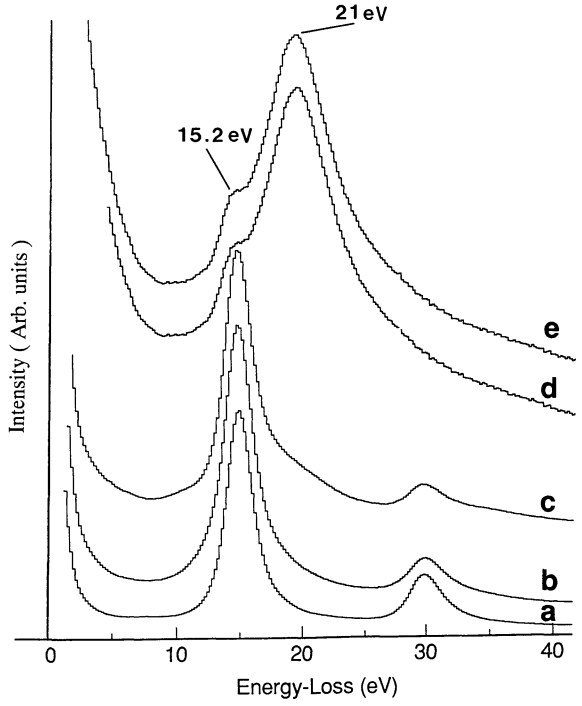

Fig. 5. — Change of plasmon loss spectra from Al during 30 kV N_2^+ ion implantation with a flux of 2×10^{18} $(N^+)/m^2s$ at 400 °C. Fluence: a) unimplanted, b) 6×10^{20}, c) 1.2×10^{21}, d) 1.8×10^{21}, e) 2.4×10^{21} $(N^+)/m^2$.

Table II. — *Summary of the experimental interplanar spacing ($d_{exp.}$-value) obtained into aluminum during nitrogen ion implantation with a flux of* 2×10^{18} *$(N^+)/m^2s$ at* 400 °C. *(hkl, Miller indices of lattice planes; hkil, Miller-Bravais indices of lattice planes; d_{th}, theoretical interplanar spacing; $d_{exp.}$, experimental interplanar spacing).*

hkl	hkil	d_{th}(nm)	Phase	d_{exp}(nm)			N/m^2
				$6x10^{20}$	$1.2x10^{21}$	$1.8x10^{21}$	$2.4x10^{21}$
001		0.3922	Al_2O_3				0.389
	$01\bar{1}0$	0.2702	AlN	0.265		0.271	0.271
	0002	0.2495	AlN	0.257	0.257	0.259	0.250
	$01\bar{1}1$	0.2376	AlN	0.244			0.236
111		0.2333	Al	0.233	0.231		0.233
(222)		0.2287	AlN_c	0.228	0.228		
012		0.2082	Al_2O_3			0.206	0.206
200		0.2021	Al				(strong)
002		0.1961	Al_2O_3				
	$01\bar{1}2$	0.1833	AlN			0.181	0.181
022		0.1737	Al_2O_3				
	$11\bar{2}0$	0.1560	AlN			0.153	0.156
233		0.1508	Al_2O_3	0.152			
220		0.1429	Al			0.144	
	$01\bar{1}3$	0.1417	AlN				
013		0.1402	Al_2O_3	0.140		0.139	0.139
(440)		0.1400	AlN_c				
023		0.1334	Al_2O_3			0.133	
	$02\bar{2}1$	0.1304	AlN	0.130	0.131	0.129	0.129
224		0.1273	Al_2O_3		0.127		
	0004	0.1247	AlN				
311		0.1219	Al				0.222
	$02\bar{2}2$	0.1188	AlN				
222		0.1167	Al		0.117	0.117	

References

[1] Morita M., Isogai S., Tsubouchi K. and Mikoshiba N., *Appl. Phys. Lett.* **38** (1981) 50.
[2] Aita C.R., *J. Appl. Phys.* **53** (1982) 1807.
[3] Pavlov P.V., Zozin E.I., Tetelbaum D.I., Lesnikov V.P., Ryshkov G.M. and Pavlov A.V., *Phys. Stat. Sol. (a)* **19** (1973) 373.
[4] Tummala R.R., *Am. Ceram. Soc. Bull.* **67** (1988) 752.
[5] Belii I.M., Komarov F.F., Tishkov V.S. and Yankovskii V.M., *Phys. Stat. Sol. (a)* **45** (1978) 343.
[6] Rauschenback (B., Kolitsch A. and Richter E., *Thin Sold Films* **109** (1983) 37.
[7] Bykov V.N., Troyan V.A., Zdorovtseva G.G. and Khaimovich V.S., *Phys. Stat. Sol. (a)* **32** (1975) 53.
[8] Furuno S., Izui K.n Ono K. and Kino T., Proc. XIth Int. Cong. on EM **II** (1986) 1297.
[9] Furuno S., Hojou K., Otsu H., Sasaki T.A., Izui K., Tuskamoto T. and Hata T., *J. Electron Microsc.* **41** (1992) 273.
[10] Ohira S. and Iwaki M., *Nucl. Instr. Meth.* **B19/20** (1987) 162.
[11] Raole P.M., Prabhawalkar P.D., Kotharl D.C., Pawar P.S. and Gogawale S.V., *Nucl. Instr. Meth.* **B23** (1987) 329.